



TITLE:

Feasibility of Cu-Al-Mn superelastic alloy bar as a self-sensor material

AUTHOR(S):

Shrestha, K. C.; Araki, Y.; Yamakawa, M.; Yoshida, N.; Omori, T.; Sutou, Y.; Kainuma, R.

CITATION:

Shrestha, K. C. ...[et al]. Feasibility of Cu-Al-Mn superelastic alloy bar as a self-sensor material. *Journal of Intelligent Material Systems and Structures* 2015, 26(3): 364-370

ISSUE DATE:

2015-01-14

URL:

<http://hdl.handle.net/2433/193667>

RIGHT:

© The Author(s) 2014. Reprints and permissions: sagepub.co.uk/journalsPermissions.nav. DOI: 10.1177/1045389X14529028. jim.sagepub.com; This is not the published version. Please cite only the published version.; この論文は出版社版ではありません。引用の際には出版社版をご確認ご利用ください。

Manuscript submitted for possible publication in Journal of Intelligent Material Systems and Structures
Feasibility of Cu-Al-Mn superelastic alloy bar as a self-sensor material by Shrestha et al.

Technical Note

Feasibility of Cu-Al-Mn superelastic alloy bar as a self-sensor material

Kshitij C Shrestha¹, Yoshikazu Araki¹, Makoto Yamakawa², Nobutoshi Yoshida¹,
Toshihiro Omori³, Yuji Sutou³ and Ryosuke Kainuma³

¹Department of Architecture and Architectural Engineering, Kyoto University, Kyoto, Japan

²Department of Architecture, Tokyo Denki University, Tokyo, Japan

³Department of Materials Science and Engineering, Tohoku University, Sendai, Japan

Corresponding author:

Yoshikazu Araki, Department of Architecture and Architectural Engineering, Kyoto University, Kyoto

615-8540, Japan.

Email: araki@archi.kyoto-u.ac.jp

*Manuscript submitted for possible publication in Journal of Intelligent Material Systems and Structures
Feasibility of Cu-Al-Mn superelastic alloy bar as a self-sensor material by Shrestha et al.*

17 **Abstract**

18 This paper examines the feasibility of Cu-Al-Mn superelastic alloy (SEA) bars as possible self-sensor
19 components, taking electrical resistance measurement as a feedback. SEA bars change their
20 crystallographic structure with phase transformation, as well as electrical resistance during
21 loading-unloading process at ambient temperature. This work studies the relationship between strain and
22 electrical resistance measurements of SEAs at room temperature. Such relationship can be used in
23 determining the state of a SMA-based structure effectively, without separate sensors, by appropriately
24 measuring the changes in electrical resistance during and after structure's loading history. Quasi-static
25 cyclic tensile tests are conducted in this paper to investigate the relationship between electrical
26 resistance and strain for a 4mm diameter Cu-Al-Mn SEA bar. It was demonstrated that linear
27 relationship with little hysteresis can be achieved up to 10% strain. The test observations support the
28 feasibility of newly developed Cu-Al-Mn SEA bars, characterize by low material cost and high
29 machinability, as a multi-functional material both for structural and sensing elements.

30

31 **Keywords**

32 Cu-Al-Mn, superelastic alloy (SEA), shape memory alloy (SMA), self-sensor, electrical resistance
33 feedback

Introduction

The interest has been increasing on the use of innovative materials as multi-functional components, that would act both as structural components as well as self-sensing components (Housner et al., 1997). Structural control and seismic applications of shape memory alloys (SMAs) to civil engineering structures have been studied by a number of researchers (Dolce et al., 2000; Ozbulut et al., 2011). Shape recovery characteristic of SMAs upon unloading without any temperature variances are called as superelasticity. Also SMAs having superelasticity are called as superelastic alloys (SEAs). Application of SEAs to civil structures has a potential to contribute both to effective structural control, with shape recovery and structural damping, and to monitoring of structural members with electric resistance feedback.

Several works have been published on the variance of electric resistance with respect to strain under variable temperature and loading conditions in Ni-Ti, Cu-Zn-Al, Ni-Ti-Cu and Cu-Al-Be SEAs (Ono, 1990; Airoidi et al., 1998; Li et al., 2005; Novak et al., 2008; Gedouin et al., 2010; Cui et al., 2010). It has been reported in the works that linear relationship can be observed between electric resistance and strain in SEAs. The variance of electric resistance is caused by transformation from the austenite to the martensite phases as well as by increase in length, and decrease in cross-section area for a bar in axial tension. However, to the authors' knowledge, Cu-Al-Be SEAs have

inferior superelasticity to Ni-Ti SEAs. Ni-Ti SEAs, on the other hand, come with high material cost and low machinability that largely limit their extensive use in practical applications.

The present study examines the feasibility of Cu-Al-Mn SEA bars as sensing devices through electrical resistance feedback. Recently, it was demonstrated that Cu-Al-Mn SEAs have shape recovery capability comparable with Ni-Ti SEAs, while Cu-Al-Mn SEAs have low material cost and high machinability (Sutou et al., 2005; Araki et al., 2011). This paper reports on quasi-static tensile tests performed to study the variation of electric resistance of Cu-Al-Mn SEA bars at room temperature.

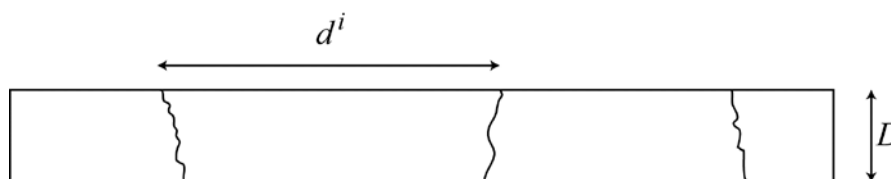
Test program

A Cu-Al-Mn SEA bar of 8mm diameter and 150mm length was prepared by Furukawa Techno Material Co., Ltd. The nominal composition of the bar is Cu-17 at.% Al-11.4 at.% Mn. The SEA bars were obtained by hot forging and cold drawing. The solution treatment was conducted at 900 °C, followed by quenching in water, and they were subsequently aged at 200°C to stabilize superelastic property. The martensite start temperature, M_s , the martensite finish temperature M_f , the austenite start temperature A_s , and the austenite finish temperature A_f of above bars are, $M_s = -74^\circ\text{C}$, $M_f = -91^\circ\text{C}$, $A_s = -54^\circ\text{C}$, and $A_f = -39^\circ\text{C}$. The original 8mm diameter

bar was threaded 20mm length at the ends to grip the rod specimen as shown in Figure 1 and the remaining central part of the rod of length, L 106mm was reduced with sectional diameter D of 4mm in order to avoid fracture at the threaded portion. Here, the relative grain size d/D , defined as the ratio between the average grain size d and the bar diameter D , is about 4, as illustrated in Figure 2. In Cu-Al-Mn SEA, superelasticity strongly depends on the relative grain size d/D , where higher recovery strain can be achieved as the relative grain size increases. Excellent superelasticity can be expected when $d/D=4$ (Sutou et al., 2005; Omori et al., 2013).



Figure 1. Photograph of an SEA bar test specimen.



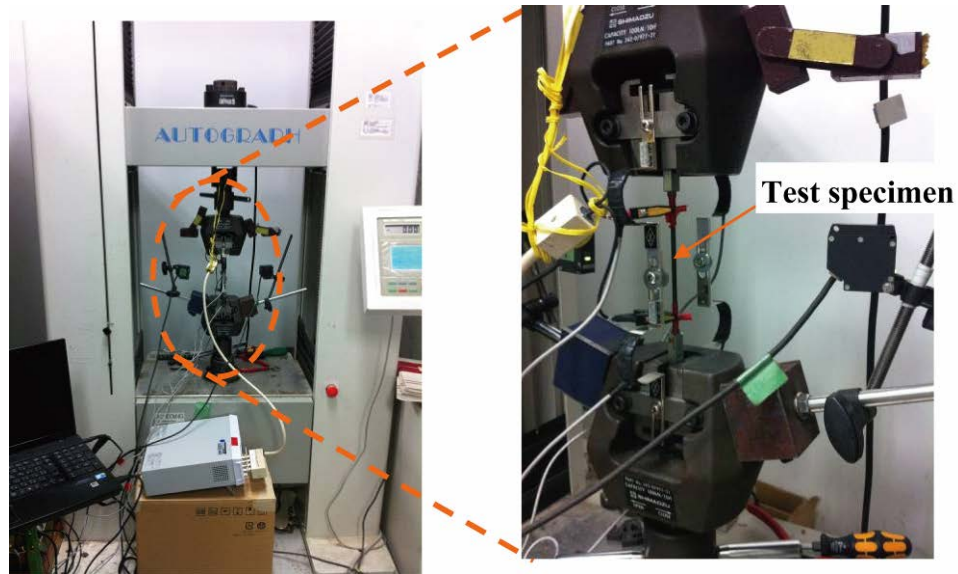
d^i — Grain size for i th grain

D — Bar diameter

Figure 2. Typical bamboo-like grain structure for Cu-Al-Mn SEA bar with relatively large grain size.

Manuscript submitted for possible publication in *Journal of Intelligent Material Systems and Structures*
Feasibility of Cu-Al-Mn superelastic alloy bar as a self-sensor material by Shrestha et al.

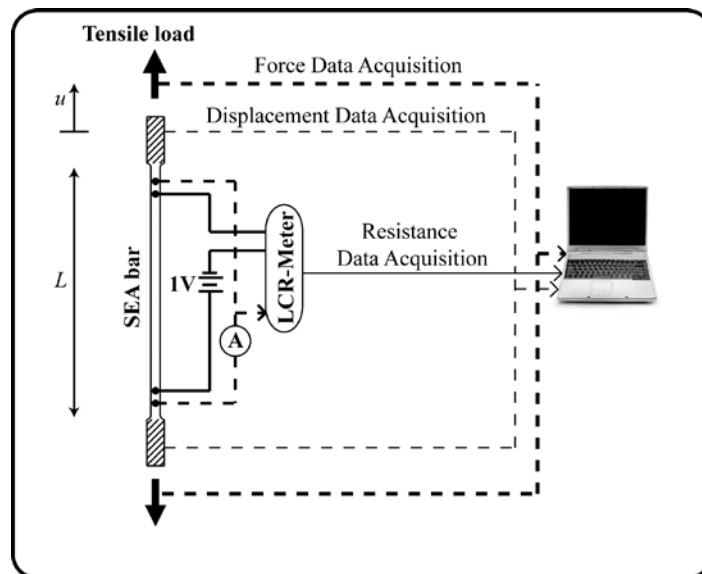
89



90

91

Figure 3. Photograph of test set-up.



92

93

Figure 4. Schematic representation of test set-up and layout.

Figures 3 and 4 show the test set-up for quasi-static tensile test with specific layout followed to measure the change in electric resistance during the loading/unloading cycle of the SEA bar specimen. Electric resistance measurements were done using LCR-Meter at 1V input voltage. Electric resistance measurements were made at the range of 100 mΩ for data acquisition. Displacement measurements were made using a set of clip-type displacement transducers (PI-gauges) attached to the cross heads as shown in Figure 3 between the cross-heads. The strain, $\epsilon = u/L$, was computed taking the change in deformation, u , restricted mainly to the reduced sectional length, L , as illustrated in Figure 4. Deformation, u , was recorded from relative displacement recorded by the PI-gauges. It should be noted here that the strain value obtained by the present technique may be slightly overestimated, which leads to underestimation of Young's modulus. Data sampling was done at 100Hz frequency.

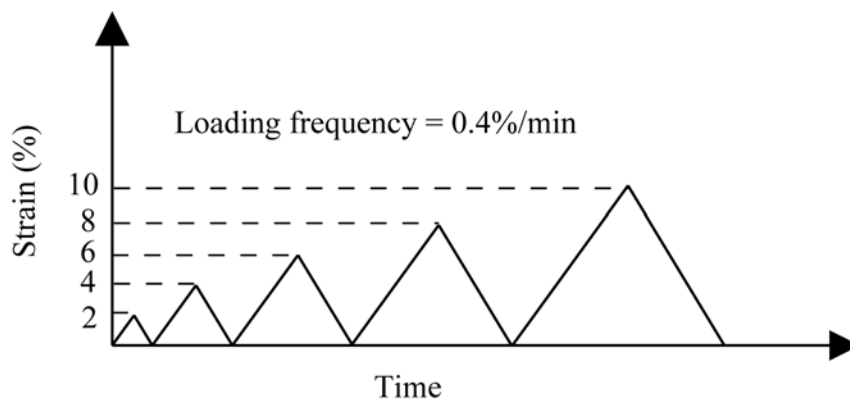


Figure 5. Loading history – Specimen was loaded to a target strain, followed by unloading to zero stress in each cycle.

The adopted loading history is shown in Figure 5. Strain was applied at the strain rate of 0.4%/min at room temperature. Five different target strain amplitudes were chosen, 2%, 4%, 6%, 8% and 10% consecutively. It should be noted only one SEA bar sample was used in all the tests.

Experimental observations

Figures 6 and 7 illustrates the results for the variation in the electric resistance and in the stress with respect to the applied strain during the quasi-static loading on the given SEA specimen. Observations for the target strain amplitudes of 2%, 4% and 6% are shown in Figure 6 and for amplitudes of 8% and 10% are consecutively shown in Figure 7. Electric resistance variation has been presented as the change in electric resistance defined by $dR=(R-R_{\text{initial}})/R_{\text{initial}}$, where R_{initial} , where R_{initial} is the resistance measured at unloaded state. It should be noted that during the tests the value of R_{initial} recorded was 2.12 m Ω .

Stress versus strain characteristics observed are shown in the left column of Figures 6 and 7. For the strain amplitudes of 2% up to 8%, the characteristic stress-strain

*Manuscript submitted for possible publication in Journal of Intelligent Material Systems and Structures
Feasibility of Cu-Al-Mn superelastic alloy bar as a self-sensor material by Shrestha et al.*

responses observed are similar, shown by typical flag-shaped hysteresis, with transformation stress of 177MPa and elastic modulus of 30GPa. Here, the transformation stress represents the stress at which the stress-induced transition from the austenite phase to the martensite phase starts to take place, and it was computed as the 0.2% offset stress. The stress plateau is clearly observed with small hysteresis, which is typical for large grain to diameter ratio value ($d/D=4$). Note here that the relatively low elastic modulus is due to the displacement measurements between grips.

Figures in the right column of Figures 6 and 7 illustrate the electric resistance versus strain characteristics for the given strain amplitudes. As shown in the figures, there was slight decrement in resistance measurement before reaching the transformation stress, where the phase transformation initiates. Then afterwards, there was a linear increment of resistance with corresponding increment in strain. Hence, a distinct region is defined for the resistance variation at the start of phase transformation. Furthermore, during the unloading process, the variation in electrical resistance followed almost the same path as during the loading process, with negligible hysteresis observed.

Manuscript submitted for possible publication in *Journal of Intelligent Material Systems and Structures*
Feasibility of Cu-Al-Mn superelastic alloy bar as a self-sensor material by Shrestha et al.

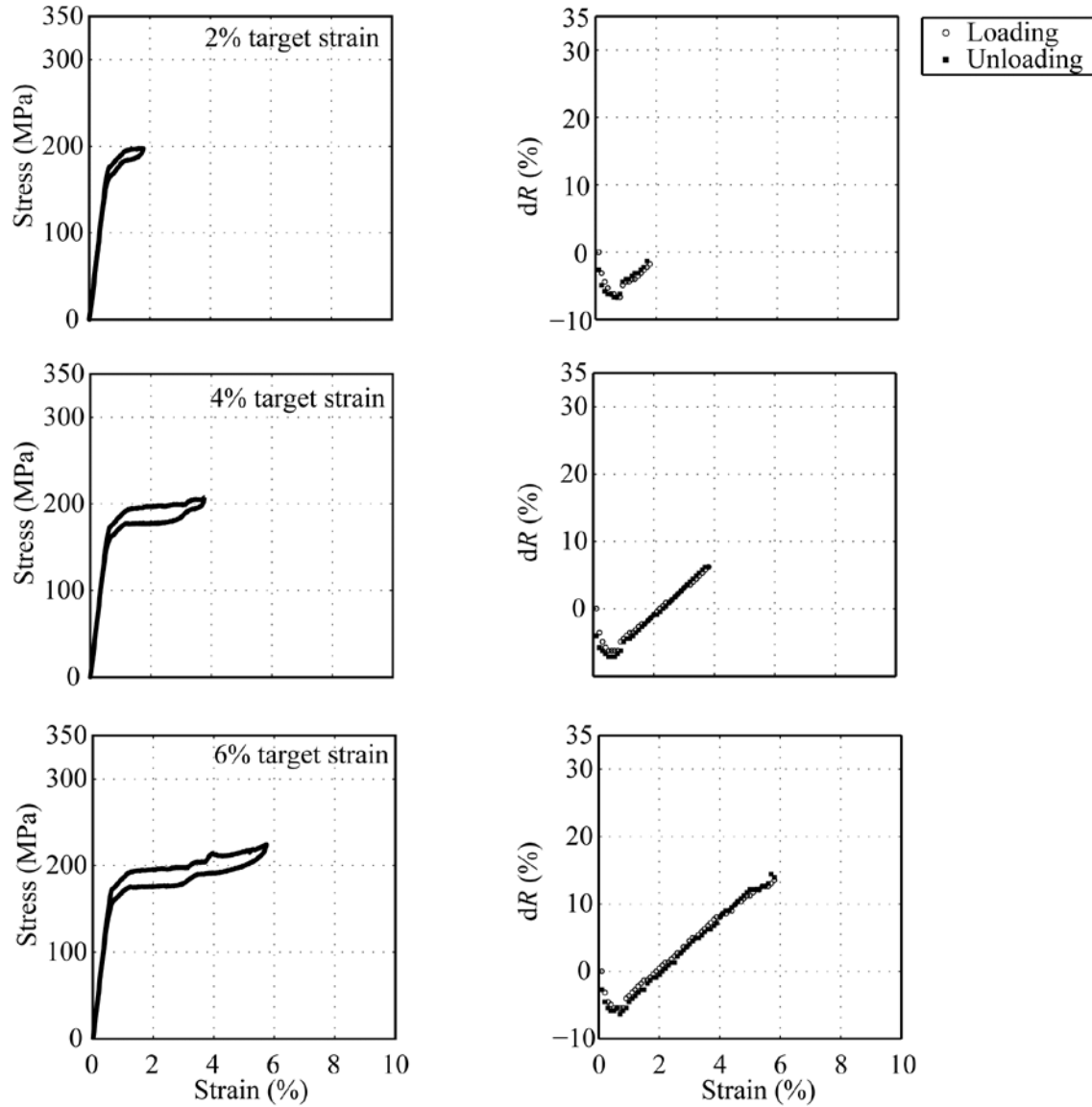


Figure 6. Experimental results for 2%, 4% and 6% target strain:

Left – Stress, σ versus strain, ε , and Right – Resistance change, dR versus strain, ε .

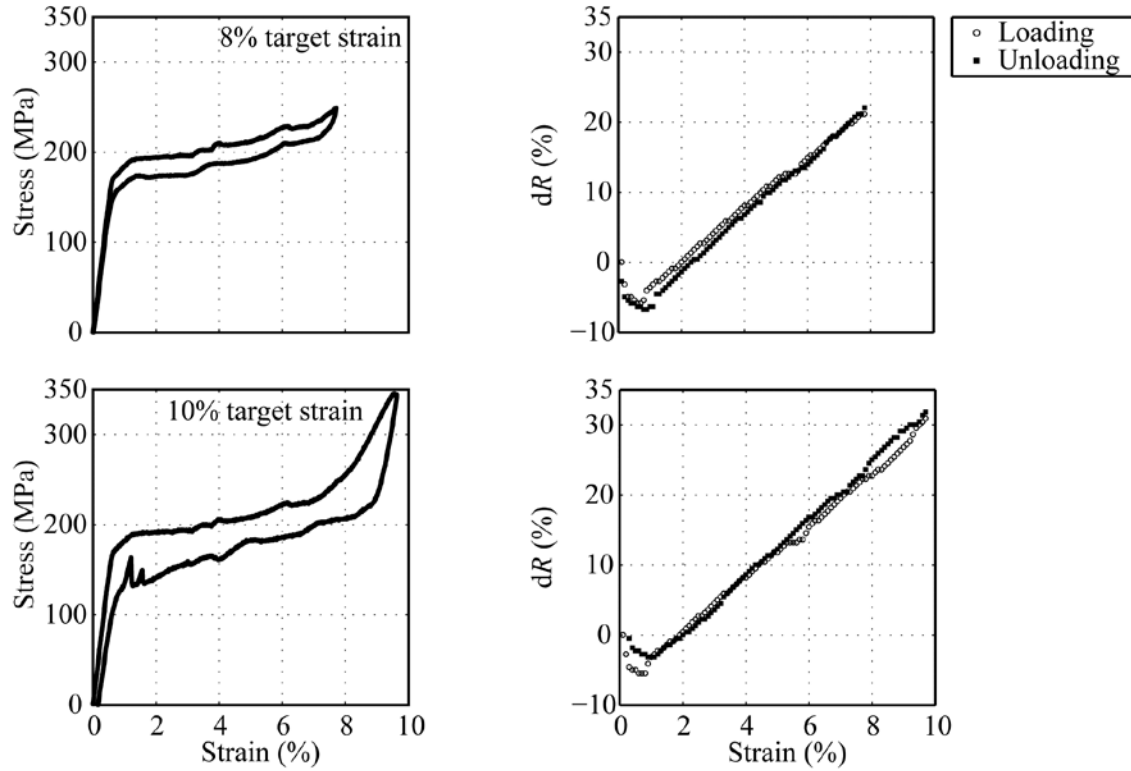


Figure 7. Experimental results for 8% and 10% target strain:

Left – Stress, σ versus strain, ε , and Right – Resistance change, dR versus strain, ε .

Discussions

Change in electrical resistance for a metal due to applied strain is represented by

$$dR = (1+2\nu) \varepsilon + d\rho \quad (1)$$

where dR is the change in electric resistance defined by $dR=(R-R_{\text{initial}})/R_{\text{initial}}$. Here,

R_{initial} is the resistance measured at the unloaded state, ε is the strain, ν is Poisson's ratio, and $d\rho$ is the change in the resistivity of the material under the applied strain given by $d\rho = \Delta\rho/\rho$, where ρ is the specific resistivity. Further details on equation (1) can be found in Cui et al. (2010).

In equation (1), the first term in the right hand side $(1+2\nu)\varepsilon$ represents effect of an increase in length, and a decrease in cross-section area for a bar in axial tension. The second term $d\rho$ represents the physical effect with change in resistivity of the material. Hence, variance in electrical resistance as observed in Figures 6 and 7 is influenced by both the geometrical effect as well as the physical effect. Geometrical effect is straight forward and largely consistent since the value of ν usually lies in the range of 0.3 to 0.45 for most metals. The resistivity term however varies greatly depending on the types of the metals (Kuczynski, 1954; Parker and Krinsky, 1963).

During experimental observations, a unique behavior of slight decrement in resistance measurement was observed before reaching the transformation stress as illustrated in Figures 6 and 7. Such observation, however, is not unique and has been documented by Airoidi et al. (1998), and Novak et al. (2008) in the elastic strain range. The initial decrement in the electric resistance is possibly contributed by the change in

resistivity of Cu-Al-Mn SEA bar. It should be noted here that for different metals and alloys, the mechanism of the change in the resistivity may be completely different, depending on its own resistivity characteristic, which requires further scrutiny.

For the strain exceeding 8% as shown in Figure 7, the slope of the stress-strain curve changes, with possible notification on transformation saturation while no residual strain appeared even when the strain is over 8%. Therefore, it is unclear whether complete phase transformation saturation occurred or not. On the other hand, the slope of electric resistance variation showed negligible difference after 8% strain value. A detailed study is required to explain more clearly on such distinctive resistance variation observed for Cu-Al-Mn SEA bars under axial tension, both in the elastic range as well as for strain exceeding 8% value, which is out of the scope of this technical note.

The performance of this Cu-Al-Mn SEA bar as a displacement transducer is measured below in terms of some basic performance characteristics, its sensitivity, hysteresis, repeatability and saturation (Murty, 2008). A measure on the sensitivity of sensor material, also defined as its gauge factor, is given by its resistance change per unit applied strain, dR/ϵ in equation (1). An average value of 3.91 sensitivity (gauge

factor) is seen which is relatively high and clearly shows the higher sensitivity characteristic of the particular SEA bar as a displacement sensor. Table 1 summarizes comparison on the sensitivity measured for different classes of SEAs, where all the SEAs show fairly effective sensitivity characteristic. It should be noted that the gauge factor is computed for the region where transformation from austenite to martensite occurs. And, it exhibits a negative gauge factor for small strain region up to 0.8% strain for Cu-Al-Mn SEAs as reported earlier due to changes in resistivity for the applied elastic strains. Hence, calibration of such SEA bar as sensor would require definition of two distinct regions, before and after the start of transformation.

As illustrated in Table 1, the previous works have been mainly done on SEAs of wire samples or thin plates. The present study involves comparatively large cross-sectional diameter Cu-Al-Mn SEA bar, tested at relatively high target strain values as compared to some of the previous works. To better understand the effect of geometrical parameters, tests on different diameters and lengths of SEA samples can be done. Such comparisons need to be done in the future works.

Table 1. Comparison on sensitivity of SEAs (in pseudoelastic regime).

SEA	Diameter/ Thickness (mm)	Temperature (°C)	Max. strain measured (%)	Sensitivity (dR/ϵ)
Ni-Ti wire (Cui et al. 2010)	0.25	70-80	8.0	3.50-3.60
Ni-Ti-Cu plate (Airoidi et al. 1998)	0.033	70-84.5	2.5	8.40
Cu-Al-Be wire (Airoidi et al. 1998)	0.80	29.3	3.0	4.80
Cu-Al-Mn bar	4.00	25.0	10.0	3.91

207

208

209 Hysteresis measures the deviation of the sensor's output signal (change in
210 resistance) at the specified point of the input signal (strain) for loading and unloading
211 states. Figure 8 illustrates the results for change in electric resistance for two opposite
212 direction loading at the same strain point. The results are close to the 45 degree dotted
213 line for all the loading cycles. The average value for difference in hysteresis
214 measurement for change in electric resistance, dR is 0.86% with standard deviation of
215 0.79%. The results show effectively lower hysteretic influence on the sensor
216 characteristics.

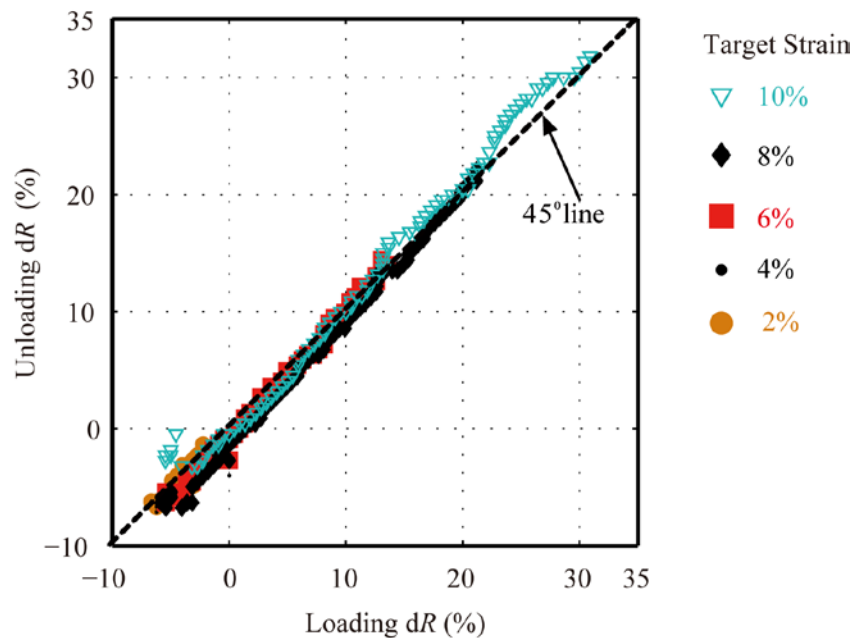


Figure 8. Performance characteristic – Hysteresis and Repeatability.

An effective repeatability characteristic is observed for this particular SEA bar, with the response for each loading cycle. The output signals of change in electric resistance for each of the consecutive loading/unloading cycles at the same strain point are relatively close to each other as shown in Figure 8. An average value for the difference in change in resistance, dR at the particular strain point when loaded at different strain amplitudes is 0.83% with standard deviation of 0.64%. The possible effect of cycling on the slope value of resistance-strain curve and also the repeatability

characteristic is an important aspect to better understand the behavior and applicability in practical applications. Wu et al. (1999) reported for NiTi wire, the slope of dR and strain remain almost same up to 20 cycles of loading, in addition to the residual strain and residual resistance accumulated with each cycle. Further study is necessary on such effect of cyclic behavior on the electric resistance of Cu-Al-Mn SEA bars.

Saturation level for a particular sensor is defined by its operating limit up to which the sensor material exhibits linear behavior and beyond this limit the output signal shows nonlinearity. The test results for the Cu-Al-Mn SEA bars as illustrated in Figures 6 and 7 show perfectly linear behavior for target strain up to 8%. Negligible nonlinearity with slight hysteresis is seen for strain beyond 8%. This shows relatively large saturation level for these particular Cu-Al-Mn SEA bars as sensor components.

With such linear increment in resistance with strain, high sensitivity, negligible hysteresis, high repeatability, and high saturation limit, the strain measurements from the electric resistance feedback is accurate enough to represent and monitor the actual strain on SEA elements. Such a self-sensor can be easily and conveniently applied to a wide range of smart civil engineering structures with proper electric resistance feedback from the embedded SEA elements, which primarily also work as structural

244 control elements.

245

246 **Conclusions**

247

248 The variation of electric resistance of Cu-Al-Mn SEA bars has been examined under
249 cyclic tension with five different target strain amplitudes of 2%, 4%, 6%, 8% and 10%.
250 Slight decrement in resistance was observed before the stress reached the transformation
251 stress. After reaching the transformation stress, linear variation of electric resistance
252 with increasing strain has been clearly observed up to 10% strain. The linear
253 relationship between the electric resistance and the strain has been also observed during
254 the unloading cycle. Furthermore, performance characteristics in terms of sensitivity,
255 hysteresis, repeatability and saturation were found excellent. The results demonstrate
256 the capability of Cu-Al-Mn SEA bars as a multi-functional component as a structural
257 element as well as a sensing element, which can be used for both structural control and
258 monitoring purposes.

259

260 **Acknowledgements**

261

262 The present research was supported by the A-STEP program (#AS2315014C) provided

Manuscript submitted for possible publication in Journal of Intelligent Material Systems and Structures
Feasibility of Cu-Al-Mn superelastic alloy bar as a self-sensor material by Shrestha et al.

by Japan Science and Technology Agency (JST). Prof. Tetsuji Matsuo of Department of Electrical and Electronic Engineering, Kyoto University provided important comments and recommendations during research meetings. All the supports mentioned above are highly acknowledged.

References

Airoidi G, Lodi DA and Pozzi M (1998) The electric resistance of shape memory alloys in the pseudoelastic regime. *Journal De Physique IV : JP* 7(5): C5-507-C5-512.

Araki Y, Endo T, Omori T, et al. (2011) Potential of superelastic Cu–Al–Mn alloy bars for seismic applications. *Earthquake Engineering and Structural Dynamics* 40(1): 107–115.

Cui D, Song G and Li H (2010) Modeling of the electrical resistance of shape memory wires. *Smart Materials and Structures* 19(5): 055019.

Dolce M, Cardone D and Marnetto R (2000) Implementation and testing of passive control devices based on shape memory alloys. *Earthquake Engineering and Strucural Dynamics* 29(7): 945-968.

Gedouin PA, Chirani SA and Calloch S (2010) Phase proportioning in CuAlBe shape

Manuscript submitted for possible publication in Journal of Intelligent Material Systems and Structures
Feasibility of Cu-Al-Mn superelastic alloy bar as a self-sensor material by Shrestha et al.

- 281 memory alloys during thermomechanical loadings using electric resistance
282 variation. *International Journal of Plasticity* 26(2): 258-272.
- 283 Housner GW, Bergman LA, Caughey TK, et al. (1997) Structural control: past, present,
284 and future. *Journal of Engineering Mechanics ASCE* 123(9): 897–971.
- 285 Kuczynski GC (1954) Effect of elastic strain on the electrical resistance of metals.
286 *Physical Review* 94(1): 61-64.
- 287 Li H, Mao CX and Ou JP (2005) Strain self-sensing property and strain rate dependent
288 constitutive model of austenitic shape memory alloy: experiment and theory.
289 *Journal of Materials in Civil Engineering* 17(6): 676-685.
- 290 Murty DVS (2008) *Transducers and Instrumentation*. New Delhi: PHI Learning
291 Private Limited.
- 292 Novak V, Sittner P, Dayananda GN, et al. (2008) Electric resistance variation of NiTi
293 shape memory alloy wires in thermomechanical tests: Experiments and simulation.
294 *Materials Science and Engineering A*, 481-482(1-2 C): 127-133.
- 295 Omori T, Kusama T, Kawata S, Ohnuma I, Sutou Y, Araki Y, Ishida K and Kainuma R
296 (2013) Abnormal grain growth induced by cyclic heat treatment. *Science*,
297 341(6153): 1500-1502.

Manuscript submitted for possible publication in Journal of Intelligent Material Systems and Structures
Feasibility of Cu-Al-Mn superelastic alloy bar as a self-sensor material by Shrestha et al.

- 298 Ono N (1990) Pseudoelastic deformation in a polycrystalline Cu-Zn-Al shape memory
299 alloy. *Materials Transactions, JIM* 31(5): 381-385.
- 300 Ozbulut OE, Hurlebaus S and Desroches R (2011) Seismic response control using shape
301 memory alloys: a review. *Journal of Intelligent Material Systems and Structures*
302 22(14): 1531-1549.
- 303 Parker RL and Krinski A (1963) Electrical resistance-strain characteristics of thin
304 evaporated metal films. *Journal of Applied Physics* 34(9): 2700-2708.
- 305
- 306 Sutou Y, Omori T, Yamauchi K, Ono N, Kainuma R and Ishida K (2005) Effect of
307 grain size and texture on pseudoelasticity in Cu-Al-Mn-based shape memory wire.
308 *Acta Materialia* 53(15): 4121-4133.
- 309 Wu XD, Wu JS and Wang Z (1999) The variation of electrical resistance of near
310 stoichiometric NiTi during thermo-mechanic properties. *Smart Materials and*
311 *Structures* 8: 574-578.